Amplification and saturation of the thermoacoustic instability in a standing-wave prime mover

Matthieu Guédra, Thibaut Devaux, Guillaume Penelet, Pierrick Lotton

ACOUSTICS 2012

Amplification and saturation of the thermoacoustic instability in a standing-wave prime mover

M. Guédra, T. Devaux, G. Penelet and P. Lotton

Laboratoire d'acoustique de l'université du Maine, Bât. IAM - UFR Sciences Avenue Olivier Messiaen 72085 Le Mans Cedex 9
matthieu.guedra.etu@univ-lemans.fr

In this paper, a thermoacoustic standing-wave device is studied, which consists of a quarter-wavelength straight resonator equipped with a 600 CPSI ceramic stack. Transient regimes leading to steady state acoustic pressure are measured under various heating conditions and for several locations of the stack inside the resonator. Experiments show interesting behaviours such as an "overshoot" for the acoustic pressure before its final stabilization, or a periodic "on-off" of the wave. A discrete time model is proposed to reproduce these transient behaviours. For each time step, the temperature distribution along the device is computed first by solving non-linear diffusion equations, then the amplification rate of the acoustic wave is calculated from the imaginary part of the resonant frequency of the system. Nonlinear saturating acoustic effects such as the thermoacoustic heat flow inside the stack and the Rayleigh's streaming in the resonator are introduced in the model, and their impact on the dynamics of wave amplitude growth are quantified. The results show good agreement between the experiments and theory, in terms of amplification process and final stabilized pressure amplitude.

1 Introduction

Thermoacoustic prime movers are acoustic resonators inside which a heterogeneously heated open-cells porous material (referred as the "stack") is responsible for the generation of spontaneous large-amplitude acoustic waves. When the temperature gradient imposed along the stack exceeds a critical value (the *onset threshold*), a self-sustained acoustic wave is amplified and saturated by non linear effects, leading to a steady state for the acoustic pressure.

The studied thermoacoustic device is a standing-wave, quarter-wavelength straight resonator, as schematically shown in Fig. 1. Though its design is very basic, the behaviour of this type of system is, by nature, strongly non-linear, and some particular exciting conditions may lead to complicated and interesting transient processes such as an "overshoot" or a periodic "on-off" of the wave.

The experimental investigations of this thermoacoustic prime mover are reported in section 2. In section 3, the theoretical model used for the description of transient regime of wave amplitude growth is presented and the results are qualitatively compared with those obtained from measurements.

2 Experiments

The thermoacoustic device, schematically drawn in Fig. 1 consists of a quarter-wavelength straight cylindrical glass pipe of length $L = 49\ cm$ and inner radius $R = 2.6\ cm$. The 600 CPSI ceramic stack made of square pores (semi-width $r_s = 0.45\ mm$) is equipped at one side with a Nichrome resistant wire. This wire is connected to a DC voltage-current source and is used to supply an amount of heat Q to the system. The length of the stack is $l_s = 4.8\ cm$. The hot side of the stack is located at $x = x_h$. A 1/4 inch condenser microphone is flush-mounted at the location of the rigid termination ($x = L$) and is connected to a standard soundcard of a computer for data acquisition.

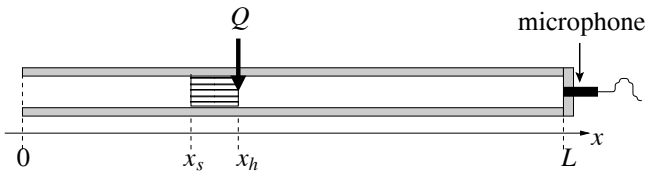

Figure 1: Schematic drawing of the standing-wave prime mover.

For particular locations of the stack inside the tube and low heat power supply, we observed periodic "switch on-off" of the acoustic wave. For example, the Figure 2-(a) shows the temporal evolution of the amplitude of acoustic pressure for $x_s = 19.2\ cm$. The onset heat power for this stack position is $Q_{onset} = 19.6W$. To obtain the Fig. 2-(a), the heat power Q has been fixed at a lower value than Q_{onset} ($Q = 18\ W$) and, after waiting the equilibrium state of heat transfer, an increment $\Delta Q = 0.16Q$ has been applied. When the increment of heat power is sufficient (e.g. $\Delta Q = 0.30Q$, Fig. 2-(c)), the "on-off" behaviour disappears and the amplitude of the acoustic pressure presents an "overshoot" (the amplitude reaches a maximum and then decreases until the stabilization).

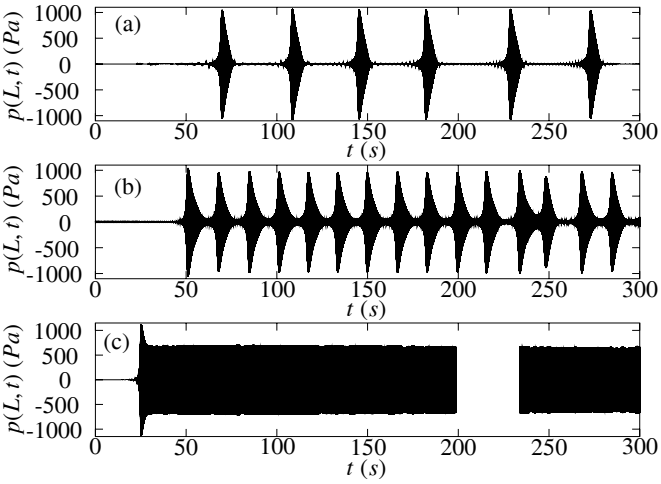

Figure 2: Temporal evolution of the acoustic pressure $p(L, t)$, for different values of the heat increment ΔQ (supplied at time $t = 0$) above the initial heat supply $Q = 18W$ (slightly below $Q_{onset} = 19.6W$). The stack position is $x_s = 19.2\ cm$. (a) $\Delta Q/Q = 16\%$, (b) $\Delta Q/Q = 24\%$,(c) $\Delta Q/Q = 30\%$.

3 Theory

3.1 Amplification coefficient

The proper description of the thermoacoustic device is made by writing the propagation of acoustic waves in the different elements of the system. The assumption of harmonic plane waves allows to write the acoustic variables as

$$p_1(x,t) = \Re\left\{\tilde{p}_1(x)e^{-i\omega t}\right\}, \tag{1}$$

for the acoustic pressure, where ω is the angular frequency and $\sim$ denotes the complex amplitude, and

$$\xi_1(x,y,t) = \Re\left\{\tilde{\xi}_1(x,y)e^{-i\omega t}\right\}, \tag{2}$$

where ξ_1 can be all of the other first-order acoustic variables which will be specified later.

With these complex notations, the three different sections of the system are treated as acoustical two-ports :

$$\begin{pmatrix} \tilde{p}_1(x_s) \\ \langle \tilde{u}_{1,x}(x_s) \rangle \end{pmatrix} = \mathbf{M_{w,1}} \begin{pmatrix} \tilde{p}_1(0) \\ \langle \tilde{u}_{1,x}(0) \rangle \end{pmatrix} \quad (3)$$

$$\begin{pmatrix} \tilde{p}_1(x_h) \\ \langle \tilde{u}_{1,x}(x_h) \rangle \end{pmatrix} = \mathbf{M_s} \begin{pmatrix} \tilde{p}_1(x_s) \\ \langle \tilde{u}_{1,x}(x_s) \rangle \end{pmatrix} \quad (4)$$

$$\begin{pmatrix} \tilde{p}_1(L) \\ \langle \tilde{u}_{1,x}(L) \rangle \end{pmatrix} = \mathbf{M_{w,2}} \begin{pmatrix} \tilde{p}_1(x_h) \\ \langle \tilde{u}_{1,x}(x_h) \rangle \end{pmatrix} \quad (5)$$

where $u_{1,x}$ is the axial component of the acoustic volume velocity. The transfer matrices $\mathbf{M_{w,1}}$, $\mathbf{M_s}$ and $\mathbf{M_{w,2}}$ appearing in Eqs. (3), (4) and (5) describe acoustic propagation in a duct or a stack with a heterogeneous temperature distribution : their analytical expressions are derived from the well-known differential equation of thermoacoustics [1]. This equation is transformed into a Volterra integral equation and the transfer matrices are written as infinite series of integral operators [see Eq. (19) in Ref. [2]].

The combination of Eqs. (3), (4) and (5) leads to the expression

$$\begin{pmatrix} \tilde{p}_1(L) \\ \langle \tilde{u}_{1,x}(L) \rangle \end{pmatrix} = \mathbf{M_{w,2}} \times \mathbf{M_s} \times \mathbf{M_{w,1}} \times \begin{pmatrix} \tilde{p}_1(0) \\ \langle \tilde{u}_{1,x}(0) \rangle \end{pmatrix} \quad (6)$$

$$= \begin{pmatrix} M_{pp} & M_{pu} \\ M_{up} & M_{uu} \end{pmatrix} \times \begin{pmatrix} \tilde{p}_1(0) \\ \langle \tilde{u}_{1,x}(0) \rangle \end{pmatrix}, \quad (7)$$

and the two conditions $\tilde{p}_1(0) = 0$ (no radiation) and $\langle \tilde{u}_{1,x}(L) \rangle = 0$ (rigid wall) are reported in Eq. (6) in order to obtain the characteristic equation of the thermoacoustic device :

$$M_{uu}(\omega, T(x)) = 0. \quad (8)$$

It is worth noting that M_{uu} is a complex quantity and solving Eq. (8) is equivalent to solving two equations with two unknown variables. A solution (ω, T) of Eq. (8) represents an operating point of the system. Rigorously, the solutions of Eq. (8) in the Fourier domain (with the assumption of a purely real angular frequency) are values for angular frequency ω and temperature $T(x)$ which describe an equilibrium point, either unstable (onset threshold) or stable (steady state), and corresponding for both cases to an acoustic wave which is neither amplified, nor attenuated.

It is however possible to describe the amplification/attenuation of the thermoacoustic instability by assuming that the system does not operate on an equilibrium state, but actually on a "quasi-steady" state [3]. To do this, we let the angular frequency be allowed to be complex,

$$\omega = \Omega + i\epsilon_g, \quad (9)$$

so that the equation (1) becomes

$$p_1(x,t) = \Re\left\{\tilde{p}_1(x)e^{-i\omega t}\right\} = e^{\epsilon_g t}\Re\left\{\tilde{p}_1(x)e^{-i\Omega t}\right\}, \quad (10)$$

meaning that the acoustic pressure is assumed to oscillate at frequency $\Omega = \Re(\omega)$, while the attenuation/growth of the sound wave is characterized by the thermoacoustic amplification coefficient ϵ_g. Under the "quasi-steady state" assumption ($\epsilon_g << \Omega$) and for a fixed temperature distribution $T(x)$ (the temperature is supposed to be constant on the time scale of few acoustic periods), it is then possible to solve Eq. (8) using conventional numerical methods to find the solution $\left(\Omega, \epsilon_g\right)$ for the angular frequency of the oscillations and the amplification rate.

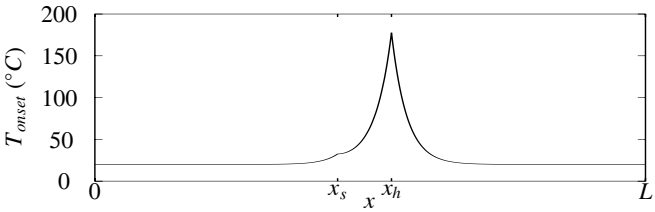

Figure 3: Spatial temperature distribution along the prime mover computed from the numerical heat transfer model for $x_s = 19.2\ cm$ and $Q_{onset} = 21.2\ W$.

3.2 Onset threshold

Solving Eq. (8) allows to compute Ω and ϵ_g for a given temperature distribution. From this statement, the stability conditions are simply reached when

$$\epsilon_g = 0. \quad (11)$$

When non-linear effects are neglected, the solution of Eq. (11) corresponds to the onset threshold of the thermoacoustic prime mover.

The temperature $T(x)$ is calculated from the knowledge of the heat power Q supplied at $x = x_h$ using an iterative finite-differences numerical scheme. When the stack is located at $x_s = 19.2\ cm$, the calculation of onset conditions gives $Q_{onset} = 21.2\ W$, instead of $Q_{onset} = 19.6\ W$ observed in experiments, and the corresponding temperature field $T_{onset}(x)$ computed with the numerical scheme is in Fig. 3.

3.3 Transient regime

Apart from the stability conditions, the coefficient ϵ_g represents the amplification rate of the thermoacoustic instability. From the consideration of Eq. (10), it is then quite direct that the time variations of the peak amplitude of the acoustic pressure, notably at the location of the microphone $P_1(t) = |p_1(L,t)|$, are described by the simple ordinary differential equation

$$\frac{dP_1}{dt} - \epsilon_g\left(T(x,t)\right)P_1(t) = 0. \quad (12)$$

The equations governing unsteady heat transfers in the thermoacoustic prime mover are presented in section 3.3.3. In these equations, the contributions of two non-linear effects are added, which are responsible for a distortion of the temperature field and for the saturation of the acoustic instability. These two effects – namely, the acoustically enhanced heat flux and the Rayleigh streaming – are described in sections 3.3.1 and 3.3.2.

3.3.1 Thermoacoustic heat flux

The first non-linear effect which is taken into account in the model is the acoustically enhanced heat flux in the stack

$$\varphi_{ac} = \frac{1}{2}\rho_0 c_0 \Re\left\{\langle \tilde{s}_1 \tilde{v}^*_{1,x} \rangle\right\}, \quad (13)$$

where ρ_0 and c_0 stand for the mean density of the fluid and the adiabatic speed of sound, respectively, s_1 is the oscillating part of the entropy, $v_{1,x}$ is the axial component of the acoustic velocity, $\langle \cdots \rangle$ denotes the average over the transverse dimension y and $*$ denotes the complex conjugate [4].

The entropy s_1 can be expressed as a function of the acoustic pressure p_1 and velocity $v_{1,x}$ by using the momentum and energy conservation equations. From the distribution of the acoustic fields along the stack, it is then possible to compute the heat flux φ_{ac} representing the heat transport in the pores of the stack due to acoustics.

3.3.2 Rayleigh streaming

In closed devices, the existence of a second-order mass flow due to large amplitude acoustic waves and effects of viscosity is often referred as "Rayleigh streaming". The interaction between a viscous fluid submitted to an acoustic wave and solid boundaries results in the development of streaming cells [6]. In heterogeneously heated system such as thermoacoustic prime movers, the existence of a steady mass flow is of great importance because it acts as a source of internal forced convection and may cause distortion of the temperature distribution.

In 2001, Bailliet *et al.* [7] proposed an analytical model for the computation of Rayleigh streaming in ducts submitted to a temperature gradient. By using a method of successive approximations in the governing equations of thermoacoustics and stating that the total mass flow through the section of the duct must be zero, it is possible to derive an expression for the axial component of the second-order time-averaged Eulerian velocity $\overline{v_{2,x}}(x, y)$, valid for cylindrical geometries [see Eq. (16) in Ref. [7]]. The axial component of the streaming velocity is then obtained as

$$\overline{V_{2,x}} = \overline{v_{2,x}} + \frac{\overline{\rho_1 v_{1,x}}}{\rho_0}. \tag{14}$$

Typical results for transverse profiles of $\overline{V_{2,x}}$ in one stack's pore and in the large resonator are shown in Figs. 4-(a) and 4-(b), respectively. Accounting for the effect of streaming in a mono-dimensional heat transfer model requires to consider the streaming cells in a very simplified way, as it is illustrated in Fig. 5-(a) : the large tube and stack sections are separated into two zones of equivalent cross sectional area (referred as the *inner* zone and the *outer* zone) in which the fluid flows at the same velocity but in opposite directions. From the calculation of the axial component $\overline{V_{2,x}}$ given by Eq. (14), it is then possible to obtain the average streaming velocity in inner and outer zones as

$$v_{str}^{(f)}(x) = \frac{2\pi}{\pi R^2} \int_0^R \left|\overline{V_{2,x}}\right| r dr, \tag{15}$$

for the large tube medium, and

$$v_{str}^{(s)}(x) = \frac{2\pi}{\pi r_s^2} \int_0^{r_s} \left|\overline{V_{2,x}}\right| r dr \tag{16}$$

for the stack medium. Finally, the temporal evolution of the streaming velocity is described by the differential equation

$$\tau^{(f,s)} \frac{dv_{str}^{(f,s)}}{dt} + v_{str}^{(f,s)} = \Gamma_v^{(f,s)} P_1^2, \tag{17}$$

where $\Gamma_v^{(f)}$ (resp. $\Gamma_v^{(s)}$) is obtained from Eq. (15) (resp. Eq. (16)) with $P_1 = 1\ Pa$ and $T(x) = T_{onset}(x)$. In Eq. (17), $\tau^{(f)}$ and $\tau^{(s)}$ are characteristic stabilization times of the acoustic streaming in the large tube and in one stack's pore, respectively, and defined as [8]

$$\tau^{(f)} = \frac{4R^2}{\pi^2 \nu} \simeq 18\ s \quad \text{and} \quad \tau^{(s)} = \frac{4r_s^2}{\pi^2 \nu} \simeq 5.10^{-3}\ s. \tag{18}$$

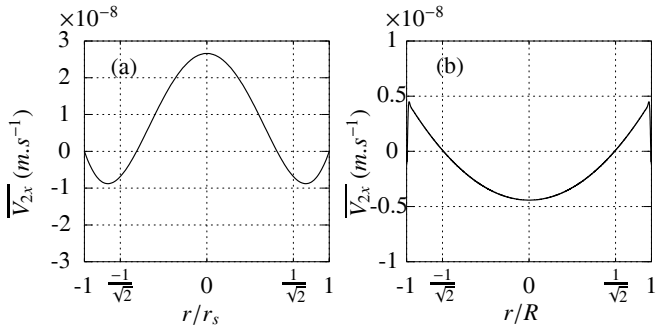

Figure 4: Transverse profiles of the acoustic streaming velocity $\overline{V_{2,x}}$ in one pore of inner radius r_s (a) and in the resonator of inner radius R (b).

Noting that the characteristic time $\tau^{(s)}$ is very small, the establishment of the streaming cells in the stack may be considered as instantaneous and Eq. (17) for the stack becomes

$$v_{str}^{(s)} = \Gamma_v^{(s)} P_1^2. \tag{19}$$

Acoustic streaming may also be responsible for heat convection at the location of the interfaces $x = x_s$ and $x = x_h$. Estimating the quantity of heat carried by the flow is a tedious task because of many strongly non-linear and badly known effects which may occur at the interface between the waveguide and the stack. However, some recent measurements of Rayleigh streaming velocity in comparable systems show that the presence of the stack modifies strongly the mass flow, notably when the stack is located at a maximum for the amplitude of streaming velocity [11]. Therefore, the acoustic streaming velocity may become very high and new convective cells may appear in the vicinity of the stack. All of these observations seem to indicate that a large amount of heat may be convected at the boundaries of the stack.

The heat taken away from an interface by the mean mass flow is estimated in a very simplified way. Considering the problem of a mean flow, initially at the temperature T_1, which goes towards a rigid interface at constant temperature T_2 (Fig. 5-(b)), the heat flux φ_{conv} is supposed to be almost equivalent to this carried away by a steady flow from an isothermal grid by unwrapping the streaming cell. With this simplified approach and after some derivations the convection flux at the interface $x = x_s$ is then estimated as

$$\varphi_{conv}(x_s) = \varphi_{conv}^{(f)}(x_s) + \varphi_{conv}^{(s)}(x_s), \tag{20}$$

with

$$\varphi_{conv}^{(f)}(x_s) = \rho_0 C_p v_{str}^{(f)}(x_s) \left(T(x_s) - T_c\right), \tag{21}$$

$$\varphi_{conv}^{(s)}(x_s) = -\Phi \rho_0 C_p v_{str}^{(s)}(x_s) \left(T(x_s) - T(x_h)\right), \tag{22}$$

where Φ is the porosity of the stack. Similarly, the convection flux at the interface $x = x_h$ is estimated as

$$\varphi_{conv}(x_h) = \varphi_{conv}^{(f)}(x_h) + \varphi_{conv}^{(s)}(x_h), \tag{23}$$

with

$$\varphi_{conv}^{(f)}(x_h) = \rho_0 C_p v_{str}^{(f)}(x_h) \left(T(x_h) - T_c\right), \tag{24}$$

$$\varphi_{conv}^{(s)}(x_h) = \Phi \rho_0 C_p v_{str}^{(s)}(x_h) \left(T(x_h) - T(x_s)\right). \tag{25}$$

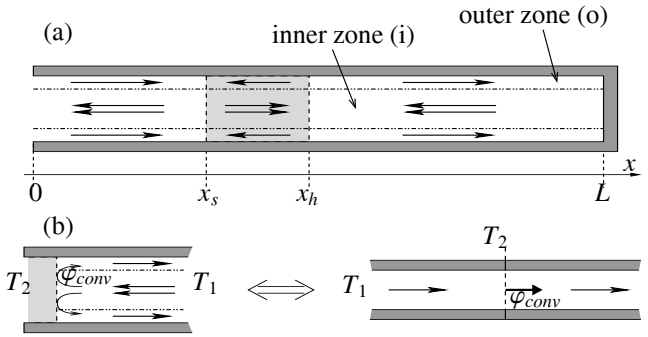

Figure 5: Schematic representation of the simplified approach used to account for acoustic streaming in the thermoacoustic system. (a) : directions of the mass flow in the inner and outer zones. (b) : estimation of the heat convected at an interface by considering the unwrapped vortex cell and the interface as an equivalent isothermal grid at constant temperature T_2 crossed by a steady flow.

3.3.3 Heat diffusion in the prime mover

The model of heat transfer is derived by writing the heat diffusion equations in the *inner* (i) and *outer* (o) zones (see section 3.3.2) for each of the three sections of the thermoacoustic system (see Eqs. (3), (4) and (5)). The walls of the resonator are supposed to be perfect thermal sinks at room temperature T_c and the stack is considered as an equivalent fluid medium of thermal conductivity

$$\lambda_s = \Phi\lambda_0 + (1-\Phi)\lambda_c \tag{26}$$

and product of density and isobaric specific heat

$$\rho_s C_s = \Phi\rho_0 C_p + (1-\Phi)\rho_c C_c. \tag{27}$$

The two sections $x \in [0, x_s]$ and $x \in [x_h, L]$ corresponding to an empty large-radius tube are described by the following equations :

$$(\rho_0 C_p)^{(i)}\frac{DT^{(i)}}{Dt} = \frac{\partial}{\partial x}\left(\lambda_0^{(i)}\frac{\partial T^{(i)}}{\partial x}\right) - h^{(i)}\left(T^{(i)} - T_c\right), \tag{28}$$

$$(\rho_0 C_p)^{(o)}\frac{DT^{(o)}}{Dt} = \frac{\partial}{\partial x}\left(\lambda_0^{(o)}\frac{\partial T^{(o)}}{\partial x}\right) - h^{(o)}\left(T^{(o)} - T_c\right) \tag{29}$$

with the convective derivatives

$$\frac{DT^{(i)}}{Dt} = \frac{\partial T^{(i)}}{\partial t} - v_{str}^{(f)}\frac{\partial T^{(i)}}{\partial x}, \tag{30}$$

$$\frac{DT^{(o)}}{Dt} = \frac{\partial T^{(o)}}{\partial t} + v_{str}^{(f)}\frac{\partial T^{(o)}}{\partial x}, \tag{31}$$

and where $h^{(i)}$ and $h^{(o)}$ are convection coefficients characterizing the transverse heat transfers between the fluid and the walls. For a steady, laminar flow [9], these coefficients can be expressed as

$$h^{(i,o)} = 3.66\frac{\lambda_0^{(i,o)}}{2R} \tag{32}$$

The section $x \in [x_s, x_h]$ corresponding to the stack medium is described by the following equations :

$$(\rho_s C_s)^{(i)}\frac{DT^{(i)}}{Dt} = \frac{\partial}{\partial x}\left(\lambda_s^{(i)}\frac{\partial T^{(i)}}{\partial x}\right) - h_s^{(i)}\left(T^{(i)} - T_c\right) - \frac{\partial\varphi_{ac}}{\partial x} \tag{33}$$

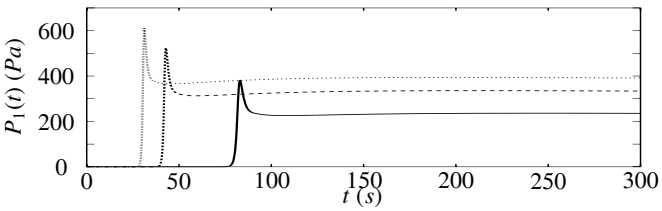

Figure 6: Temporal evolution of the acoustic pressure $P_1(t)$, for different values of the heat increment ΔQ (supplied at time $t = 0$) above the initial heat supply $Q = 19.5W$ (slightly below $Q_{onset} = 21.2W$). The stack position is $x_s = 19.2\ cm$. $\Delta Q/Q = 16\%$ (—), $\Delta Q/Q = 24\%$ (−−) , $\Delta Q/Q = 30\%$ (· · ·).

$$(\rho_s C_s)^{(o)}\frac{DT^{(o)}}{Dt} = \frac{\partial}{\partial x}\left(\lambda_s^{(o)}\frac{\partial T^{(o)}}{\partial x}\right) - h_s^{(o)}\left(T^{(o)} - T_c\right) - \frac{\partial\varphi_{ac}}{\partial x} \tag{34}$$

with the convective derivatives

$$\frac{DT^{(i)}}{Dt} = \frac{\partial T^{(i)}}{\partial t} + \Phi\frac{(\rho_0 C_p)^{(i)}}{(\rho_s C_s)^{(i)}}v_{str}^{(s)}\frac{\partial T^{(i)}}{\partial x} \tag{35}$$

$$\frac{DT^{(o)}}{Dt} = \frac{\partial T^{(o)}}{\partial t} - \Phi\frac{(\rho_0 C_p)^{(o)}}{(\rho_s C_s)^{(o)}}v_{str}^{(s)}\frac{\partial T^{(o)}}{\partial x} \tag{36}$$

and where $h_s^{(i)}$ and $h_s^{(o)}$ are coefficients characterizing transverse conductive transfers in the ceramic frame and transverse convective transfers into the pores. These coefficients are expressed considering the thermic resistance of a cylinder, so that their analytical expression is written as

$$h_s^{(i,o)} = \frac{\lambda_{s,\perp}^{(i,o)}}{\ln(2)R}, \tag{37}$$

where $\lambda_{s,\perp}$ represents an equivalent transverse thermal conductivity of the stack.

Moreover, the following boundary conditions are imposed at $x = 0$ and $x = L$

$$T^{(i)}(0) = T^{(o)}(0) = T^{(i)}(L) = T^{(o)}(L) = T_c, \tag{38}$$

and continuity equations are added at the interface $x = x_s$ and $x = x_h$, which are the continuity of temperature between the inner and outer zones

$$T^{(i)}(x_s) - T^{(o)}(x_s) = 0, \tag{39}$$

$$T^{(i)}(x_h) - T^{(o)}(x_h) = 0, \tag{40}$$

and the continuity of averaged heat flux

$$\lambda_s\,\partial_x T|_{x_s^+} - \lambda_f\,\partial_x T|_{x_s^-} + \varphi_{conv}(x_s) - \varphi_{ac}(x_s) = 0, \tag{41}$$

$$\lambda_s\,\partial_x T|_{x_h^+} - \lambda_f\,\partial_x T|_{x_h^-} + \varphi_{conv}(x_h) - \varphi_{ac}(x_h) = \frac{Q}{\pi R^2} \tag{42}$$

Solving the heat diffusion equations (28), (29), (33) and (34) combined with the appropriate boundary conditions and continuity equations permits to calculate the temporal evolution of the temperature $T(x,t)$. This is realized numerically by using a Crank-Nicholson algorithm [10].

3.3.4 Results

Finally, the computation of the temperature $T(x)$ at time t (and thus the amplification coefficient by solving Eq. (8))

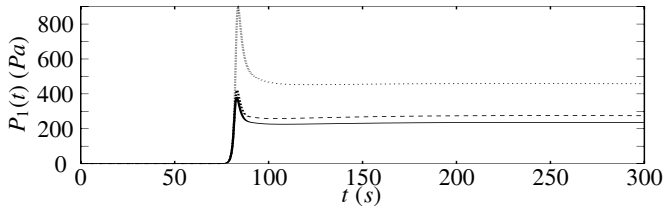

Figure 7: Temporal evolution of the acoustic pressure amplitude $P_1(t)$ for a heat increment $\Delta Q/Q = 16\%$ supplied at time $t = 0$ above the initial heat supply $Q = 19.5W$ (slightly below $Q_{onset} = 21.2W$). The stack position is $x_s = 19.2\ cm$. (—) : both thermoacoustic heat flux and streaming are taken into account ; (−−) : thermoacoustic flux only ; $(\cdots)$: acoustic streaming only.

permits to calculate numerically the amplitude of acoustic pressure from Eq. (12) and streaming velocities from Eqs. (17) and (19) at time $t + dt$. The equation (12) is solved using a fourth-order Runge-Kutta method with a varying time step, based on Richardson extrapolation. The equation (17) is solved using a simple explicit Euler method.

The Figure 6 presents the temporal evolution of the acoustic pressure amplitude P_1 with heating conditions close to those applied in experiments (see Fig. 2-(a)). The initial condition for acoustic pressure is $P_1(t = 0) = 10^{-8}\ Pa$. The model reproduces qualitatively the behaviour of the transient regimes, as well as the "overshoot" effect before stabilization. The final stabilized pressure levels are lower than those measured, which could mean that the heat supply is actually higher in experiments. Another important point is that the model cannot reproduce the "on-off" behaviour of the wave for low heat increments.

The first heat condition ($\Delta Q/Q = 16\%$ with $Q = 19.5W$, slightly below $Q_{onset} = 21.2W$) has also been investigated when both non-linear effects are taken into account separately, in order to compare their respective influences on the saturation process. The results presented in Figure 7 shows that both thermoacoustic flux and acoustic streaming seem to be responsible for an "overshoot" effect. It also appears clearly that the thermoacoustic flux is responsible for the largest part of the wave saturation. However, comparing the final pressure amplitudes for the different cases, both of the non-linear effects seem to be important and the acoustic streaming cannot be considered as negligeable in front of the thermoacoustic flux. Moreover, with the very simplified approach developped in the present model (notably for the estimation of the heat convection at the interfaces), one can resonably think that the effect of streaming is minimized in comparison with what happens in the actual device.

4 Conclusion

A simple standing-wave quarter-wavelength thermoacoustic prime mover has been studied. The experimental observations showed interesting behaviours such as an "overshoot" of the acoustic wave before stabilization, and sometimes a periodic "switch on-off" for particular conditions concerning the stack location in the resonator and the heat power supplied to the stack. We proposed a model for the reproduction of this transient regimes. The temperature distribution is computed from the derivation of heat transfers along the thermoacoustic system and some non-linear effects are added, which can cause distortion of the temperature field. Then, from the instantaneous calculation of the temperature, the amplification/attenuation coefficient is obtained by solving the characteristic equation of the system, and is used to compute the temporal evolution of the acoustic pressure. This model is able to reproduce qualitatively the transient regimes observed in experiments, notably the "overshoot" behaviour. However neither the thermoacoustic heat flux, nor the acoustic streaming seem to be responsible for the periodic "switch on-off" of the acoustic wave.

Acknowledgments

The authors are indebted to Hélène Bailliet from the Pprime Institute (UPR 3346) for helpful discussions about the modeling of acoustic streaming, and to Denis Bruneau from the I2M laboratory (UMR CNRS 5295) for helpful discussions about the modeling of heat transfer.

References

[1] G.W. Swift. Thermoacoustic engines. *J. Acoust. Soc. Am.*, 84(4):1145–1180, 1988.

[2] G. Penelet, S. Job, V. Gusev, P. Lotton and M. Bruneau. Dependence of sound amplification on temperature distribution in annular thermoacoustic engines. *Acust. Acta Acust.*, 91(3):567–577, 2005.

[3] M. Guedra and G. Penelet. On the use of a complex frequency for the description of thermoacoustic engines. *accepted for publication in Acust. Acta Acust.*

[4] A. Tominaga. Thermodynamic aspects of thermoacoustic theory. *Cryogenics*, 35(7):427–440, 1995.

[5] W.P. Arnott, H.E. Bass, and R. Raspet. General formulation of thermoacoustics for stacks having arbitrarily shaped pore cross sections. *J. Acoust. Soc. Am.* 90(6):3228–3237, 1991.

[6] S. Boluriaan and P.J. Morris. Acoustic streaming: from Rayleigh to today. *Intern. Journ. of Aeroacoustics* 2(3):255–292, 2003.

[7] H. Bailliet, V. Gusev, R. Raspet, and R.A. Hiller. Acoustic streaming in closed thermoacoustic devices. *J. Acoust. Soc. Am.*, 110(4):1808–1821, 2001.

[8] M. Amari, V. Gusev, and N. Joly. Temporal Dynamics of the Sound Wind in Acoustitron. *Acust. Acta Acust.*, 89(6):1008–1024, 2003.

[9] A.-M. Bianchi, Y. Fautrelle, and J. Etay. *Transferts thermiques*. Presses Polytechniques et Universitaires Romandes, 2004

[10] M.N. Ozisik. *Finite difference methods in heat transfer*. CRC Press, 1994

[11] S. Moreau, H. Bailliet, and J.-C. Valière. Effect of a stack on Rayleigh streaming cells investigated by laser Doppler velocimetry for application to thermoacoustic devices. *J. Acoust. Soc. Am.*, 125(6):3514–3517, 2009.